

## Current sensing in BLDC motor application

### Introduction

The brushless DC motor is very popular in industrial automation, automotive, medical and health care appliances thanks to its high reliability and lifespan. While its cost reduces every day, on contrary electronics to drive it keeps more and more important, as well as a precise and fast current sensing to ensure a multiple feedback, which can be used to determine speed, angle and the rotation direction.

In this application note, some different techniques to sense the current are met, with a focus on the inline phase current. It needs dedicated current sensing ICs, which are able to work with common mode largely higher than the power supply, and with a good and fast answer to fast common mode step variation.

This document handles the current measurement in BLDC motors for a three-phase topology described in the simplified schematic in the [Figure 2. Step mode drive](#).

## 1 How does it work?

Before facing the current measurement of a BLDC motor, it would be interesting to understand the functional principles. BLDC motors are “synchronous” devices, this means that stator flux (and thus motor phase currents) must be kept synchronous with rotor position which, as a result, must always be known.

In order to get the motor run, the magnetic generated by the stator must be checked, by taking into account the current flowing into the motor phase. A current feedback has to be as fast and precise as possible, so to control the motor phase current.

Rotor position and speed have to be known in order to achieve the synchronism. The BLDC driver powers sequentially the stator winding giving an electric field which, in its turn, makes the rotor run. In order to guarantee an efficient drive, the winding must be powered at the right time. The schematic below describes a 6-step mode drive.

**Figure 1. Current in winding A, B, C**

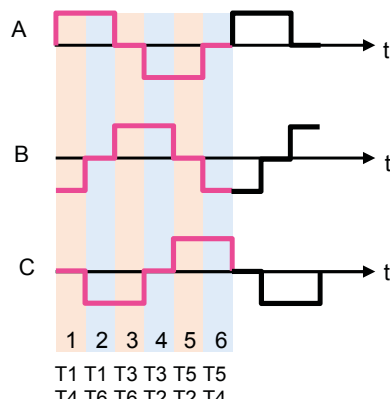
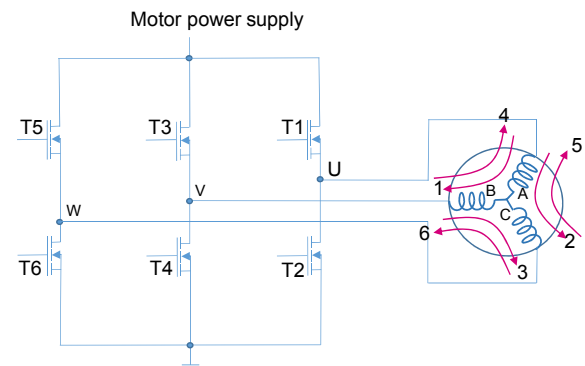


**Figure 2. Step mode drive**



During one electrical cycle, there is always one winding biased in one direction and another in the other direction. In the first step, the transistor T1 and T4 are close, the current flows through the winding A and B, in this manner the rotor moves to 60 °. In the next step the transistor T1 and T6 are closed. The current flows through the winding A and C and the rotor moves to more than 60 °.

Some of BDLC motors have the hall sensor embedded in the motor. The main function of the hall sensor is to know the rotor position to be able to energize the right winding for a good commutation sequence.

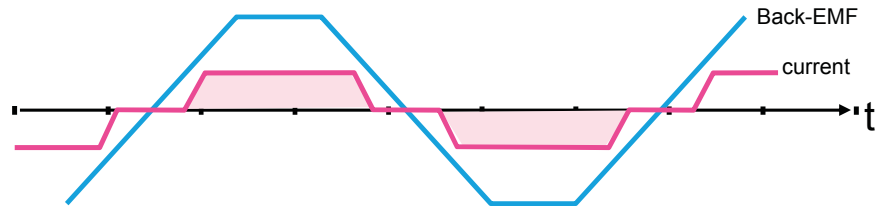
In order to simplify the motor building, or for application working in dusty and oily environment, some of BLDC motors are sensorless, therefore no hall sensor is integrated to detect the motor position.

In this case other techniques can be used to feedback information about the motor. One of them uses the back electromotive force (back-EMF) effect. This technique uses the zero-crossing of the BEMF to know the rotor position.

The back EMF is a voltage occurring in the opposite direction to current flow as a result of the motor coils moving to a magnetic field and it is proportional to the speed of the rotor.

One of the main drawbacks of the back-EMF measurement is when the motor runs to low speed or stop, and no information is provided to determine the motor position.

The maximum efficiency is achieved if the commutation between two consecutive steps is performed only when the rotor is in the right spatial position, which occurs when the BEMF signal and the phase current are synchronized.

**Figure 3. Correlation between current and back-EMF**

If current and back-EMF are not in phase, then the BLDC does not run efficiently or stops.

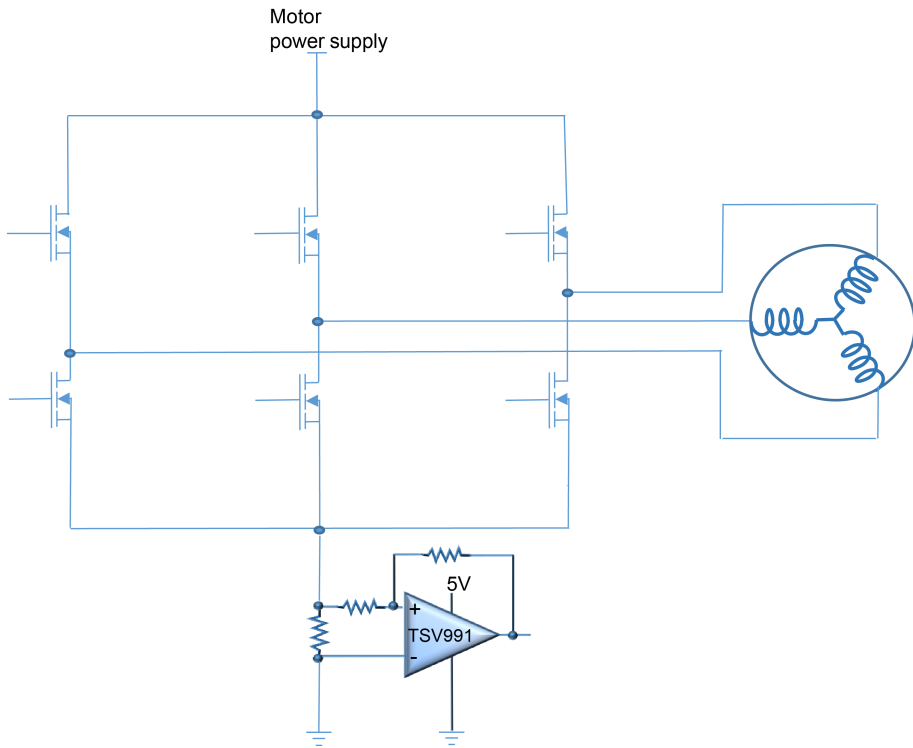
Therefore the current in such application has to be sensed.

Vector controls, also called field oriented control (FOC) is another algorithm used to check this kind of motor. It is a mathematical technique used to achieve a decoupled control of the flux and torque in a three-phase machine. It is a high-end technique but it is more and more popular. This kind of algorithm is based on a fine control of the motor currents, which have to be sensed in real time, and with accuracy to an optimized motor control. There are four different techniques to monitor the current in a BDLC application, each of them with different pros and cons.

## 1.1

### Low-side global current sensing

The simplest topology is described by the figure below, it is a global low-side current sensing. The main advantage of this technique is that the common mode voltage is close to ground allowing a wide choice of low voltage op-amp to be used. Besides, the low cost makes this technique a very interesting solution.

**Figure 4. Low-side global current sensing configuration**

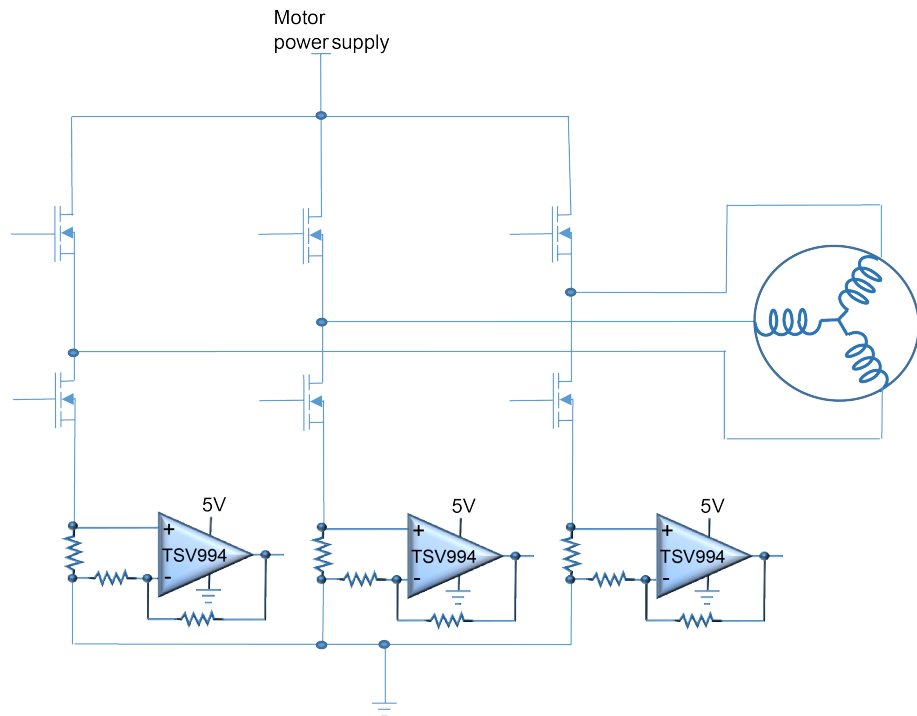
It is generally chosen when a certain fault must be detected. As it is a low-side technique, it cannot allow a shortcut to ground detection and thus motor failure. Moreover, the measured current does not necessarily match the current really flowing through the motor. In order to identify the phase current in this location, a very high slew rate op-amp is required as well as a very complex algorithm to handle this information, which is in contrast with the expected low cost solution. The TSX9291 op-amp can be used at least with gain of 2 for this kind of configuration. Besides, the TSV991 can be used at least with gain of 4 for applications with a power supply Vcc lower than 5 V.

## 1.2

### Low-side current sensing in each leg of the current driver

Comparing the 3-shunt low-side technique with the previous version allows a better approach of the phase current flowing into the motor even if it is not an exact equivalent. The low-side configuration allows the use of low power op-amp as the common mode is close to ground. However, this current measurement is sensible to ground variation, and does not detect shortcut to ground. This topology is largely used in FOC.

**Figure 5. Low-side current sensing in each leg of the current driver**



The third current measurement branch is optional and can be calculated in the controller. The TSX9291 op-amp can be used at least in gain of 2 for this kind of configuration. The TSV991 can be used at least in gain of 4 for applications with a power supply Vcc lower than 5 V.

This topology is described in detail in the AN4076.

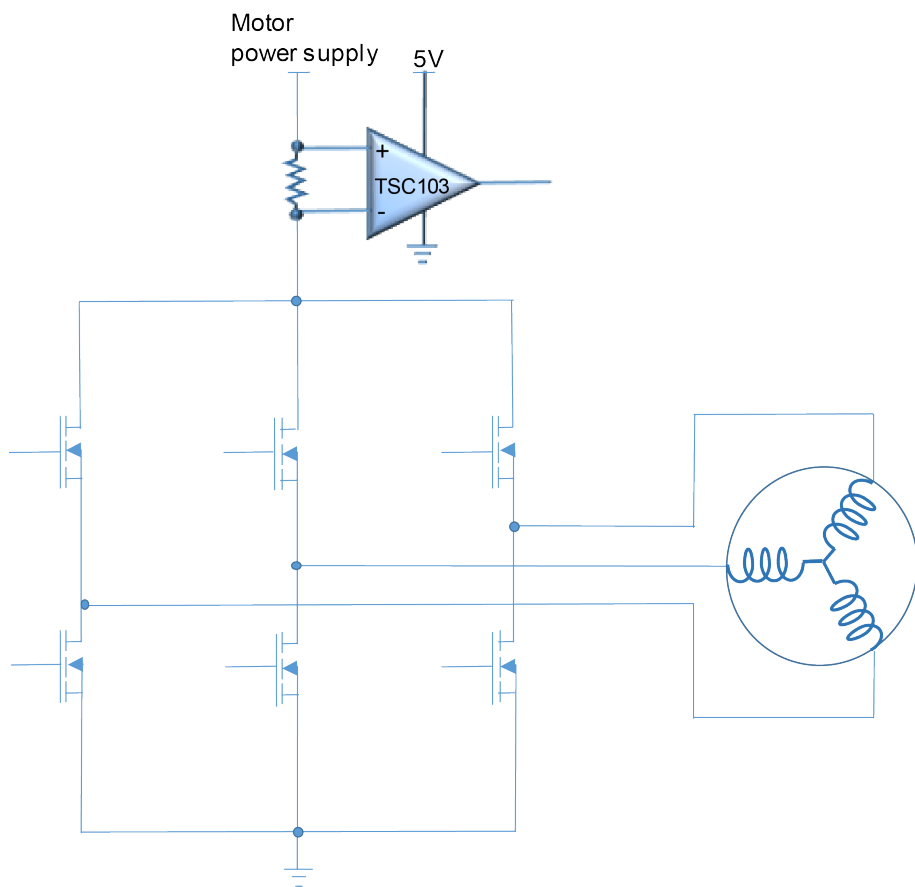
## 1.3

### High-side current sensing

Unlike the previous configurations, this one detects the shortcut to ground, and since it places close to the supply, the current measurement is not sensitive to ground disturbance. This configuration needs a special op-amp that can work with high voltage common mode inputs. In this configuration the input common mode voltage is quite stable, and the amplifier does not require any special care regarding fast common mode voltage variation.

Nevertheless, the current, which is measured, in this case does not match exactly the phase current flowing into the motor.

**Figure 6. High-side current sensing**



The TSC103 can be used in a high-side current sensing.

By combining the topology depicted in [Figure 6. High-side current sensing](#) and [Figure 4. Low-side global current sensing configuration](#), the leakage is detected by making the difference between the low-side and the high side current measurement.

## 1.4

### Inline phase current

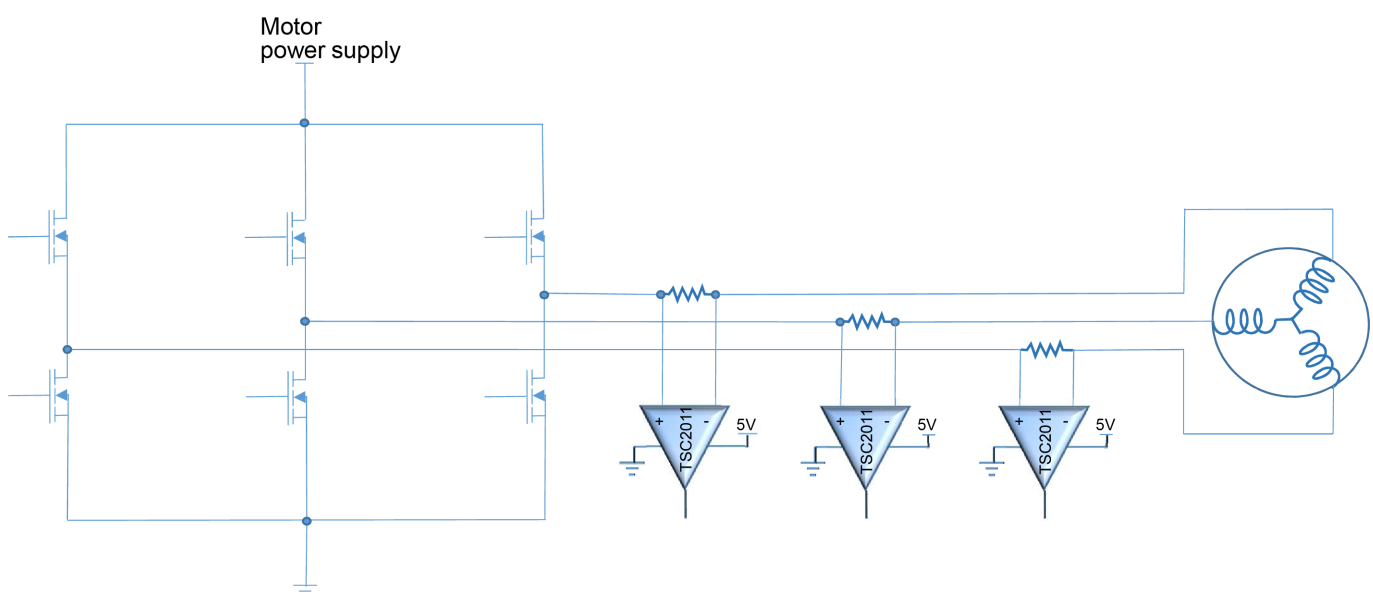
The configuration described in [Figure 7](#). **Inline phase current sensing** is the best method to know precisely the phase current flowing into the motor.

This current measurement offers the best information that can be used in feedback motor control, in order to optimize the motor performance.

As the shunt resistance is placed directly in line with the PWM driver, it uses a dedicated current sensing, which rejects the fast common mode variation.

The input pins of the current sensor can see in few nano-seconds several tens of volt, depending of the motor to drive. The current sensor should be able to reject this variation, and limit the unwanted disturbance on the output as much as possible.

**Figure 7. Inline phase current sensing**



The TSC2011 is a bidirectional high-side current sensing and can be used in such configuration.

This topology can only be used in the vector control and it is more for high-end motor controls requiring a precise current phase measurement as the case for electric power steering, or eTurbo application.

The main advantage of this topology is that the current can be read without a strong linkage to the PWM status and without timing limitations in case of very small PWM applied to the phase (low-side current sensing can only be executed while the low-side transistor of that leg is on). It also allows the detection of phase short-circuits.

## 1.5

### The TSC2011 in BDLC motor application: inline phase current topology

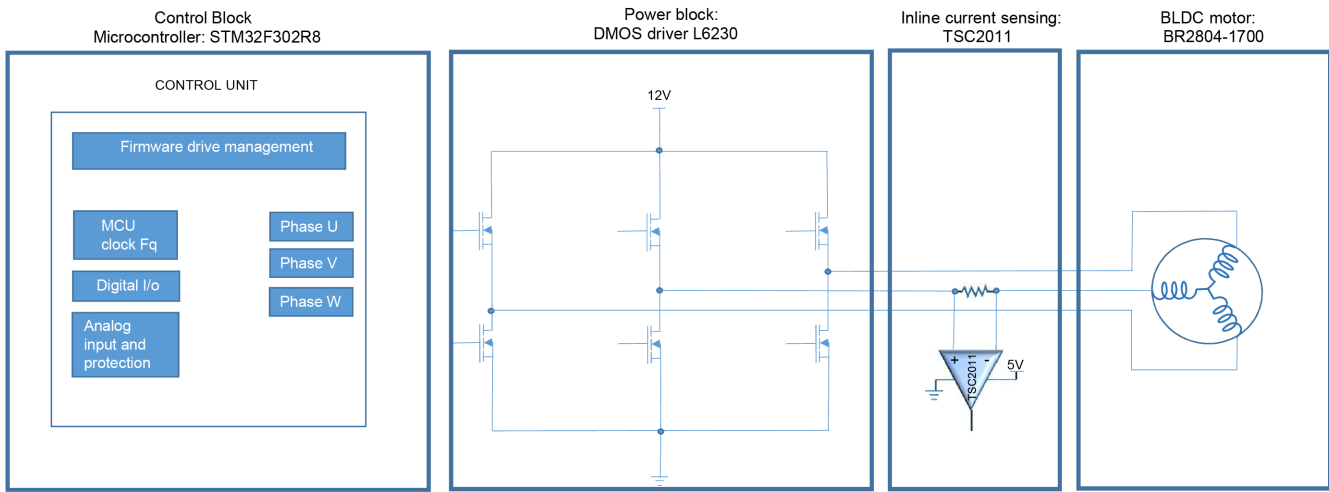
The TSC2011 provides an extended input common range from -20 V below negative supply voltage, and up to 70 V allowing either low-side or high-side current sensing, while the TSC2011 devices can operate from 2.7 to 5.5 V. Moreover, the TSC2011 has been specially designed to support fast common mode voltage variation and offers good accuracy, in order to provide a current picture as close as possible to the reality.

## 1.6

## The application description

The motor control system can be depicted in four main blocks (see [Figure 8. Overall system architecture](#)).

**Figure 8. Overall system architecture**



**Control block:** its main task is to accept user commands and drive a motor. The microcontroller STM32F302R8, provides all digital signals to properly implement motor driver control.

**Power block:** it is based on three-phase inverter topology. The core of the power block is the L6230 DMOS driver, which contains all the necessary active power and analog components to perform low voltage motor control.

**Motor:** the motor use in this application is a low voltage three-phase BLDC motor BR2804-1700 powered with 12 V.

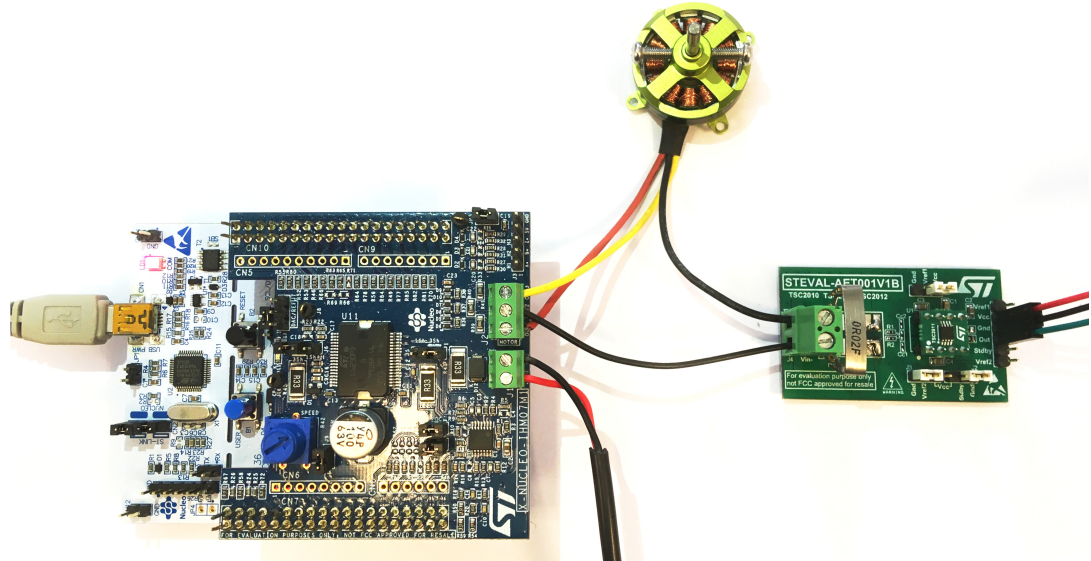
**Shunt + inline current sensing:** A shunt of 20 mΩ with 1% accuracy has been used and a TSC2011 current sensing in order to measure the current in one phase of the motor.

The ST Nucleo kit X-NUCLEO-IHM07M1 combined with the dedicated software ST motor control workbench has been used to drive the motor. The purpose of this setup is to demonstrate the TSC2011 performance in motor application control and not to develop the full algorithm.

It provides an affordable and easy-to-use solution for driving three-phase brushless DC motor.

To measure the current, the evaluation board STEVAL-AET001VB has been used with a TSC2011 current sensing (gain 60) and a shunt of 20 mΩ.

More information about this Nucleo kit, and the TSC2011 evaluation board STEVAL-AETKT1V1 are available on the ST web site.

**Figure 9.** Application system**Component choice:**

- Shunt resistor

The selection of the shunt resistor is a tradeoff between dynamic range and power dissipation.

Generally, in high current sensing application, the main focus is to reduce as much as possible the power dissipation ( $I^2R$ ) by choosing the smallest value of shunt.

Generally, the current full scale ( $I_{max}-I_{min}$ ) defines the shunt value thanks to the full output voltage range, the gain of the TSC2011. The TSC2011 offers the possibility to work with full scale  $\Delta V_{out} = 100 \text{ mV}$  to  $V_{cc}-100 \text{ mV}$  with maximum gain accuracy of 0.3%.

At first order the full current range to measure through  $R_{sense}$  can be defined by the Eq. (1), just by taking the gain error and input offset voltage as inaccuracy parameters:

$$I_{sense\_full\_scale} * R_{sense} = \frac{V_{cc} - 200 \text{ mV}}{TSC\_Gain(1 + Eg)} - 2 |V_{io}| \quad (1)$$

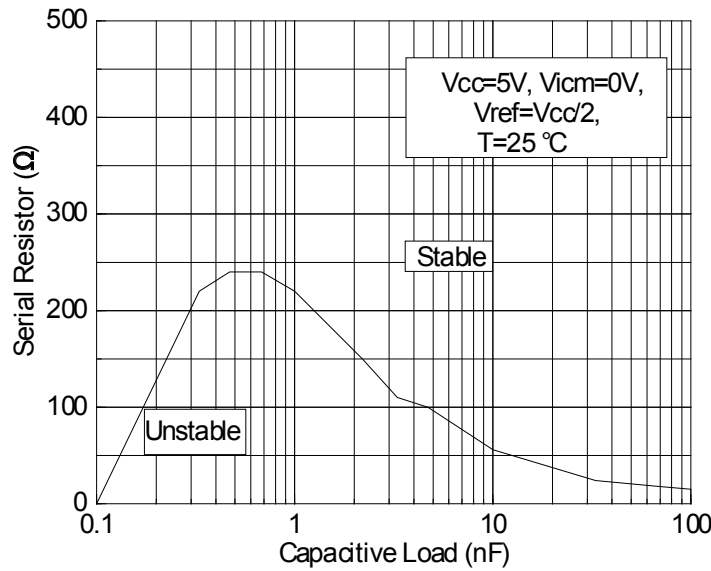
In this typical application, the TSC2011 is supplied with 5 V and the maximum current that the BLDC motor can deliver is 2.8 A. The shunt value can be reduced if the TSC2011 can be increased (ex: TSC2012), but for the same  $V_{io}$  the accuracy is reduced.

- Output RC filter

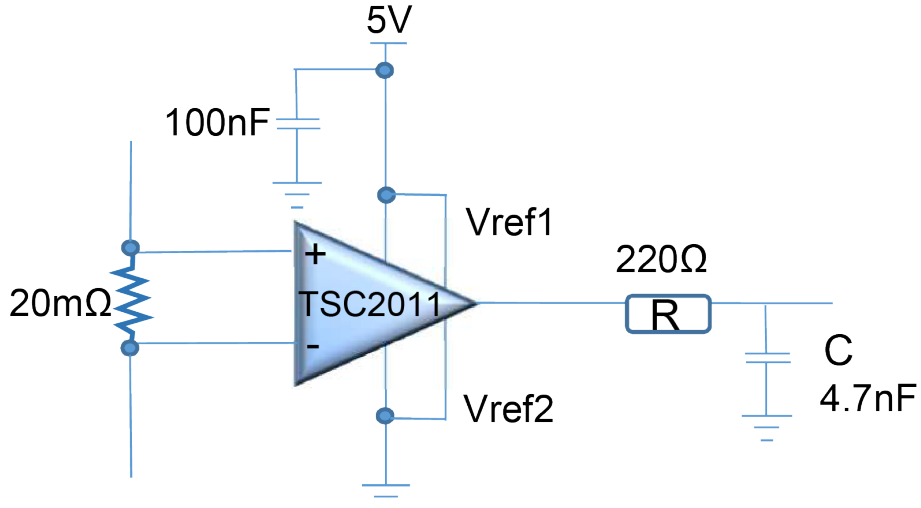
ADCs get their signal thanks to a sample and hold the capacitor. If, before a sampling, this capacitance is fully discharged, a fast and large current load can appear on the output of the TSC2011 during the sampling and hold phase. The effect of the ADC sampling and hold can be easily smoothed thanks to an RC filter on the TSC2011 output as suggested by the schematic below [Figure 11. The TSC2011 configuration](#). The capacitor of the external filter must be chosen much higher than the internal ADC capacitor, in order to easily absorb the sudden voltage variation on the output due to the sampling and hold the ADC. The resistance must be chosen according to the application speed of the system in order not to impact the whole application. The main advantage of using an RC filter is to have an antialiasing system.

The RC filter allows the bandwidth and so the noise to be limited. In this application, the PWM, by driving the motor, is set at 20 kHz. The bandwidth of the TSC2011 is 750 kHz and in this case, it might not be necessary to keep a so large frequency range. The capacitance is chosen at 4.7 nF. A special care must also be taken on the value of the added external capacitor. In fact, if this one is chosen with an excessive value and the serial resistance with a too small value, the instability on the output of the TSC2011 is a possible risk.

[Figure 10. Stability criteria with a serial resistor at VCC= 5 V](#) shows the serial resistors that must be added to the output, to make a system stable. The chosen criteria to ensure the stability of the system is an overshoot lower than 24%.

**Figure 10.** Stability criteria with a serial resistor at VCC= 5 V

To ensure a sufficient bandwidth and have good system stability a  $220\ \Omega$  resistance is used, resulting in cut-off frequency of 154 kHz.

**Figure 11.** The TSC2011 configuration

## 1.7

### Theoretical maximum error calculation

The principal sources of error that can be seen on the output of the TSC2011 are mainly due to input offset voltage, gain error and common mode rejection ratio. In addition, the shunt resistance accuracy should be taken into account. The maximum total error expected on the output of the device can be described as the sum of these different sources. The different error of the total output voltage can be written as follows:

$$V_{out} = G \left( 1 + \varepsilon G + \left| \frac{dG}{dT} \right| * |\Delta T| \right) * \left( R_{shunt} \left( 1 + \varepsilon_{shunt} \right) * (I_{sense}) + \left( V_{io} + \left| \frac{dV_{io}}{dT} \right| * |\Delta T| \right) + \left( \frac{|V_{icm} - 12V|}{CMRR} \right) + \left( \frac{V_{ref1} + V_{ref2}}{2} \right) * (1 + \varepsilon_{ref}) + Noise \right) \quad (2)$$

In Eq. (2), the maximum  $V_{io}$  value is the one of the electrical characteristics of the datasheet when the  $V_{icm}=12$  V, so 500  $\mu$ V maximum at 25 °C.

In this typical application the input common voltage varies between ground and 12 V (PWM driving the BLDC motor). From the above Eq. (2), when the input common voltage is 12 V, the error due to the CMRR is null. When the  $V_{icm}=0$  V, the CMRR error must be taken into account and the equation, indicating the output voltage with all the maximum error terms, is the following:

$$V_{out\_max} = G \left( 1 + \varepsilon G + \left| \frac{dG}{dT} \right| * \Delta T \right) \cdot \left( R_{shunt} \cdot (1 + \varepsilon_{shunt}) \cdot (I_{sense}) \right) \\ + \left( V_{io} + \left| \frac{dV_{io}}{dT} \right| * \Delta T \right) + \left( \frac{|V_{icm} - 12V|}{CMRR} \right) + \left( \frac{V_{ref1} + V_{ref2}}{2} \right) \cdot (1 + \varepsilon_{ref}) + Noise \quad (3)$$

In this Eq. (3) the maximum  $V_{io}$  value is the one of the electrical characteristics of the datasheet when the  $V_{icm}=1$  V, so 200  $\mu$ V maximum at 25 °C.

It is important to note that this calculus has been done by using all the maximum values and all the errors have been added each other, therefore the chance of getting this worst case condition is extremely low, and the error in the most part of application is largely smaller.

Note that the input bias currents are not taken into account in Eq. (3).

The linearity represents 0.03% of error only, therefore in this calculus it is absent because it is negligible. Nevertheless, as the gain error has been calculated thanks to the best fit line approach, it gives the information that the gain error can be relatively constant through the whole linear range of the TCS2011.

The noise can be then expressed as two terms, the former related to the 1/f noise and the latter due to the white noise. As the noise is bandwidth-dependent, higher the bandwidth of the application, higher the noise, so, in order to limit the impact of the noise on the output, a first order output filter of 154 kHz has been used. It is developed thanks to a resistance  $R=220$  Ω and a capacitor  $C=4.7$  nF.

The RMS value of the output noise given in  $V_{RMS}$  is the integration of the spectral noise over this 154 kHz bandwidth can be expressed by the equation below:

$$nRMS = \sqrt{\int_{0.1}^{10000} \left( \frac{100 \cdot 10^{-9}}{\sqrt{\frac{f}{1 \cdot 10^3}}} \right)^2 df + \int_{0.1}^{154000} \frac{\pi}{2} (29 \cdot 10^{-9})^2 df} * Gain \quad (4)$$

In this typical case study, the noise represents 1 mV<sub>RMS</sub> on the output.

Here is a table summarizing all the maximum error terms, using the TSC2011 at  $V_{icm}=12$  V and at  $V_{icm}=0$  V.

**Table 1. Maximum error on the output when the  $V_{icm}=12$  V @25 °C**

Error source	Calculus	Output voltage error
Gain error	$60 * V_{sense} * 0.3\%$	$60 * V_{sense} * 0.3\%$
$V_{io}$ error	$60 * 500 \mu V$	30 mV
CMRR error	$60 * \frac{12V - 12V}{\frac{90}{1020}}$	0
$V_{ocm}$ error	$2.5(1 + 0.1\%)$	2.5 mV
Noise	$60 * \sqrt{1kHz * (\ln(10k) - \ln(0.1)) * \left(\frac{100nV}{\sqrt{Hz}}\right)^2 + (154kHz * \frac{\pi}{2} - 0.1Hz) * \left(\frac{29nV}{\sqrt{Hz}}\right)^2}$	1 mV <sub>rms</sub>
Shunt resistor	$60 * V_{sense} * 1\%$	$60 * V_{sense} * 1\%$

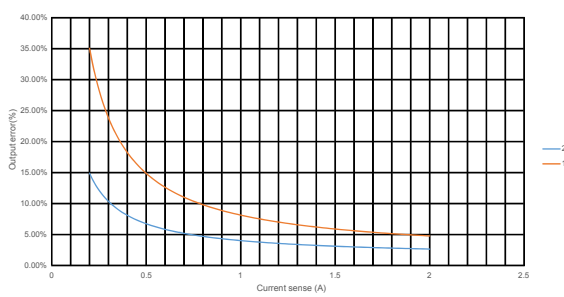
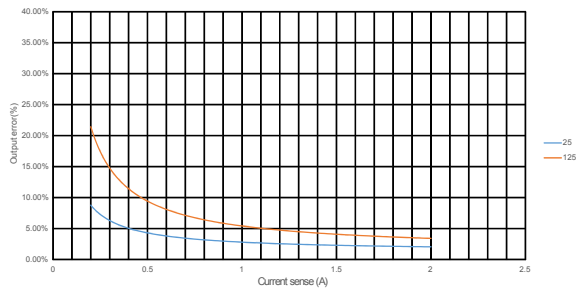
**Table 2. Maximum error on the output when the  $V_{icm}=0$  V @25 °C**

Error source	Calculus	Output voltage error
Gain error	$60*V_{sense}*0.3\%$	$60*V_{sense}*0.3\%$
$V_{io}$ error	$60*200\mu V$	12 mV
CMRR error	$60*\frac{0V - 1V}{\frac{90}{1020}}$	1.9 mV
$V_{ocm}$ error	$2.5(1 + 0.1\%)$	2.5 mV
Noise	$60*\sqrt{1kHz*(\ln(10k) - \ln(0.1)) * \left(\frac{100nV}{\sqrt{Hz}}\right)^2 + \left(154kHz*\frac{\pi}{2} - 0.1Hz\right) * \left(\frac{29nV}{\sqrt{Hz}}\right)^2}$	$1\text{ mV}_{rms}$
Shunt resistor	$60*V_{sense}*1\%$	$60*V_{sense}*1\%$

Both [Figure 12. Total error vs current @ \$V\_{icm}=12\$  V](#) and [Figure 13. Total error vs current @ \$V\_{icm}=0\$  V](#) express the maximum total error on the output versus the current flowing into the motor phase. These curves are a graphical representation of the [Eq. \(2\)](#) and [Eq. \(3\)](#), where the input voltage offset, the input offset voltage drift, the gain error, the CMRR error, the output common mode voltage error, and the accuracy of the shunt resistance are involved. It represents a worst case condition, since the maximum parameter of the datasheet is considered, and as all errors have been summed up, the chance of getting this level of inaccuracy is extremely low.

The [Figure 12. Total error vs current @ \$V\_{icm}=12\$  V](#) and [Figure 13. Total error vs current @ \$V\_{icm}=0\$  V](#) represent the total error in % on the output at ambient and 125 °C, for  $V_{icm}=12$  V and  $V_{icm}=0$  V, by using a shunt of 20 mΩ at 1% and a current flowing into one motor phase in the range of [0.2 to 2 A].

Note that  $V_{ref}$  is set to  $V_{cc}/2$ , the current from 0. A to 2 A has been plotted only. The symmetrical graphs would apply for negative current.

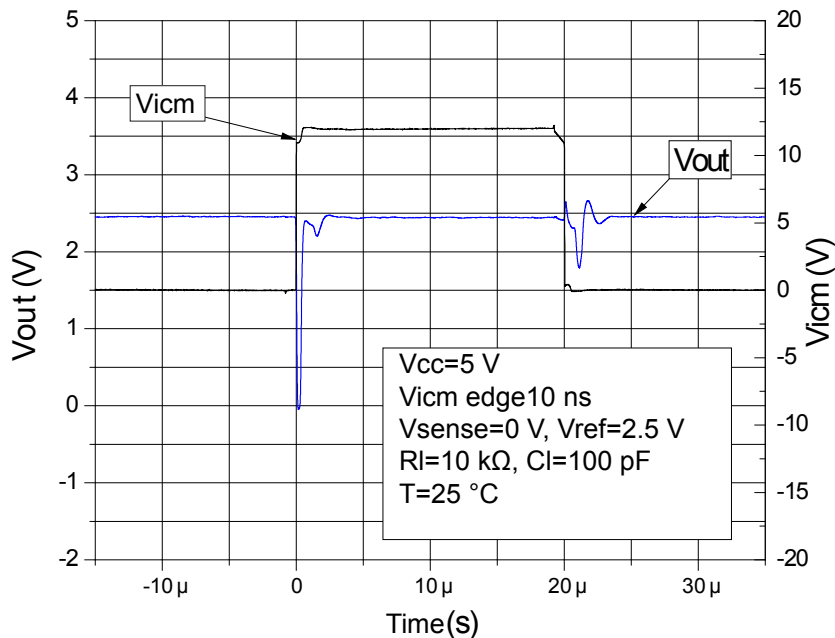
**Figure 12. Total error vs current @ $V_{icm}=12$  V****Figure 13. Total error vs current @ $V_{icm}=0$  V**

## 1.8 Fast common mode rejection

One of the main advantages of the TSC2011 current sensing product is its good and fast output answer to quick variation of the input common voltage.

The [Figure 14. 12 V common mode step response](#) shows that the output requires less than 5 µs to recover after a common mode step variation of 12 V within 5 ns.

Figure 14. 12 V common mode step response



## 1.9

### The TSC2011 in motor application

The [Figure 15. Behavior of the output of the TSC2011 in a motor application](#) shows the response of the TSC2011 in the application described by [Figure 7. Inline phase current sensing](#).

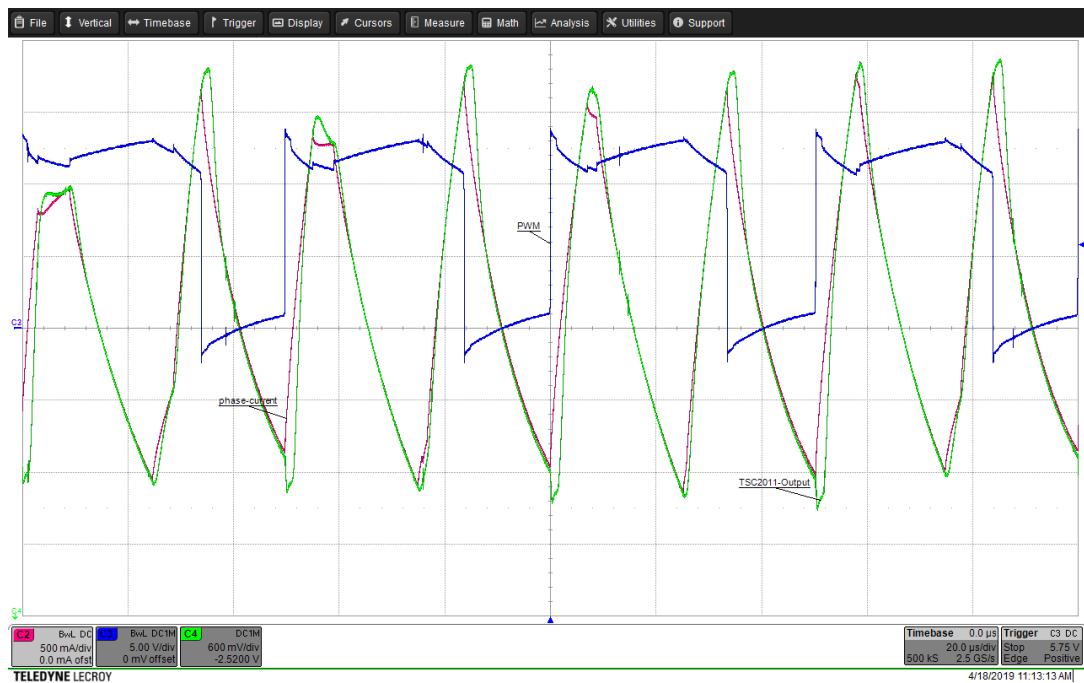
Only one phase current motor out of three has been measured.

The PWM frequency of the motor is 20 kHz, represented by the blue curve in [Figure 15. Behavior of the output of the TSC2011 in a motor application](#).

The current flowing in one phase of the motor is in the range of 2.5 A, for a 7000 rpm motor speed.

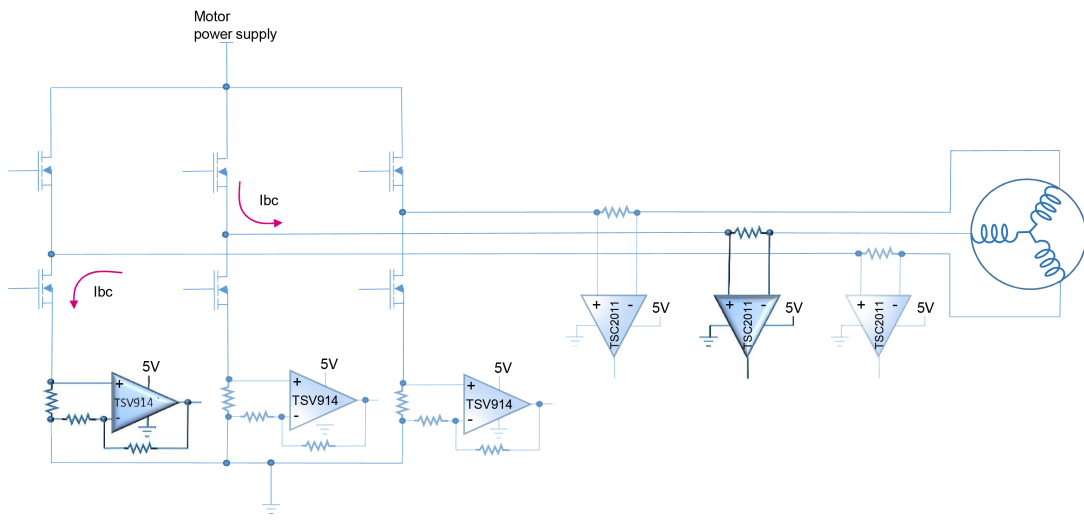
The pink curve is issued from a current probe placed on the same phase as the shunt resistance. The green curve represents the output of the TSC2011, after the RC filter (154 kHz), and shows the good signal integrity of the TSC2011. The pink and green curves can be superposed thus the TSC2011 provides an accurate signal for the motor control.

On the fast transition of the current a response time of less than 5  $\mu\text{s}$  can be observed, due to the TSC2011 response time to a fast common mode transition and the RC filter constant time.

**Figure 15.** Behavior of the output of the TSC2011 in a motor application

## 1.10 Comparison of low-side and inline current sensing

This section compares low-side and inline phase current sensing. The test has been done as described by the [Figure 16. Comparison with low-side and inline current sensing](#), by comparing the output of the TSC2011 and the TSV914, which represents the voltage information about the current  $I_{bc}$  flowing into the motor.

**Figure 16.** Comparison with low-side and inline current sensing

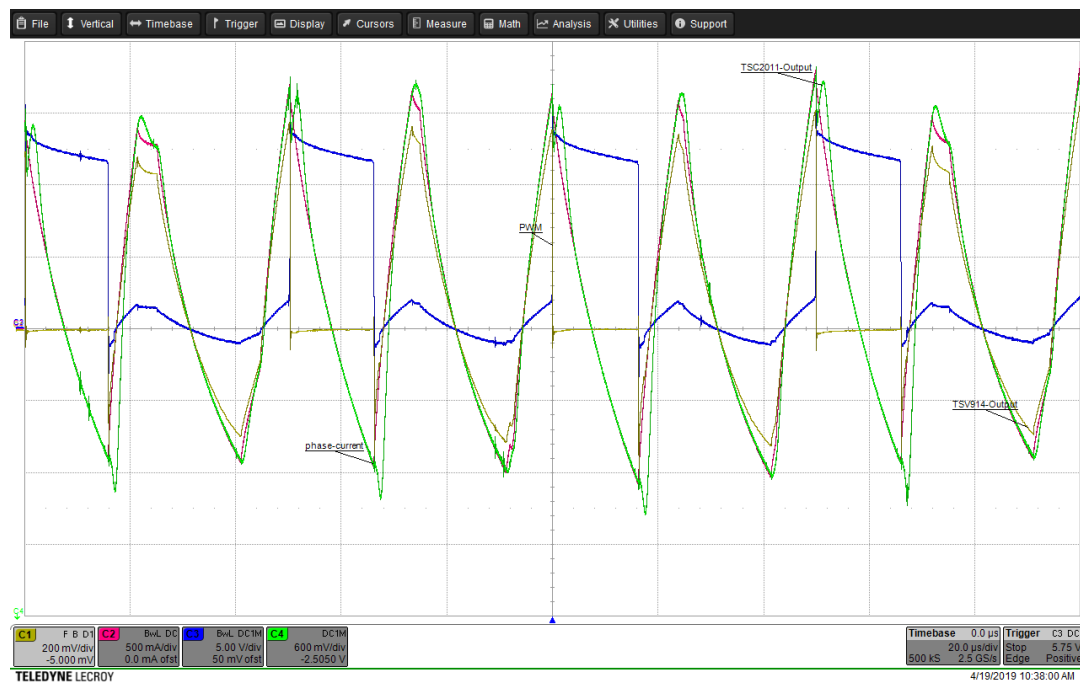
In low-side current sensing approach, developed thanks to the TSV914 op-amp, the sampling of the currents must be performed when the corresponding low-side switch is turned on, as indicated in [Figure 17. Comparison of low-side and high-side inline current phase](#) when the  $PWM=0$ .

When  $PWM=12$  V, no information about the current flowing into a phase motor can be feedbacked with low-side current sensing.

The yellow curve depicted the probing of the TSV914 output. The information is available only when the low-side transistor is ON.

Alternatively, with high-side inline configuration, the current measurement can be done during the entire PWM cycle. The output of the inline current sensing, the TSC2011 in green follows the current flowing into the phase motor (pink curve monitored thanks to a current probe).

Figure 17. Comparison of low-side and high-side inline current phase



## 1.11 Conclusion

In motor control applications, the measurement of the current is fundamental to provide a feedback on the motor. Several topologies can be used to develop this current sensing, with pros and cons.

A low-side approach can be easily developed thanks to the TSV91x or TSV99x (gain>4), with the advantage of an easy implementation and a cheaper solution.

In some automotive applications, the motor is directly mounted on the chassis of the car. In this case there is no possibility to insert a shunt between the motor and ground and so it is not possible to use a low-side current sensing topology.

In this case, a high-side current sensing could be the solution as it is less intrusive than low-side current sensing. If an accurate measurement of the phase current is critical as for example for electric power steering or e-turbo application, or application where functional safety is a must, inline current sensing can be a very good solution. The TSC2011, a bidirectional current sensing with a wide common range, is a good choice for these kind of applications, thanks to its good response time to a fast step variation on the input common mode voltage.

## Revision history

**Table 3. Document revision history**

Date	Version	Changes
20-Jan-2020	1	Initial release.

## Contents

<b>1</b>	<b>How does it work?</b>	<b>2</b>
1.1	Low-side global current sensing . . . . .	3
1.2	Low-side current sensing in each leg of the current driver . . . . .	4
1.3	High-side current sensing . . . . .	5
1.4	Inline phase current . . . . .	6
1.5	The TSC2011 in BDLC motor application: inline phase current topology . . . . .	6
1.6	The application description . . . . .	7
1.7	Theoretical maximum error calculation . . . . .	9
1.8	Fast common mode rejection . . . . .	11
1.9	The TSC2011 in motor application . . . . .	12
1.10	Comparison of low-side and inline current sensing . . . . .	13
1.11	Conclusion . . . . .	14
	<b>Revision history</b> . . . . .	<b>15</b>

## List of tables

<b>Table 1.</b>	Maximum error on the output when the $V_{icm}=12\text{ V}$ @ $25^\circ\text{C}$ .	10
<b>Table 2.</b>	Maximum error on the output when the $V_{icm}=0\text{ V}$ @ $25^\circ\text{C}$	11
<b>Table 3.</b>	Document revision history	15

## List of figures

<b>Figure 1.</b>	Current in winding A, B, C .....	2
<b>Figure 2.</b>	Step mode drive .....	2
<b>Figure 3.</b>	Correlation between current and back-EMF .....	3
<b>Figure 4.</b>	Low-side global current sensing configuration.....	3
<b>Figure 5.</b>	Low-side current sensing in each leg of the current driver.....	4
<b>Figure 6.</b>	High-side current sensing .....	5
<b>Figure 7.</b>	Inline phase current sensing .....	6
<b>Figure 8.</b>	Overall system architecture .....	7
<b>Figure 9.</b>	Application system .....	8
<b>Figure 10.</b>	Stability criteria with a serial resistor at VCC= 5 V .....	9
<b>Figure 11.</b>	The TSC2011 configuration .....	9
<b>Figure 12.</b>	Total error vs current @Vicm=12 V .....	11
<b>Figure 13.</b>	Total error vs current @Vicm=0 V .....	11
<b>Figure 14.</b>	12 V common mode step response .....	12
<b>Figure 15.</b>	Behavior of the output of the TSC2011 in a motor application .....	13
<b>Figure 16.</b>	Comparison with low-side and inline current sensing .....	13
<b>Figure 17.</b>	Comparison of low-side and high-side inline current phase.....	14

**IMPORTANT NOTICE – PLEASE READ CAREFULLY**

STMicroelectronics NV and its subsidiaries ("ST") reserve the right to make changes, corrections, enhancements, modifications, and improvements to ST products and/or to this document at any time without notice. Purchasers should obtain the latest relevant information on ST products before placing orders. ST products are sold pursuant to ST's terms and conditions of sale in place at the time of order acknowledgement.

Purchasers are solely responsible for the choice, selection, and use of ST products and ST assumes no liability for application assistance or the design of Purchasers' products.

No license, express or implied, to any intellectual property right is granted by ST herein.

Resale of ST products with provisions different from the information set forth herein shall void any warranty granted by ST for such product.

ST and the ST logo are trademarks of ST. For additional information about ST trademarks, please refer to [www.st.com/trademarks](http://www.st.com/trademarks). All other product or service names are the property of their respective owners.

Information in this document supersedes and replaces information previously supplied in any prior versions of this document.

© 2020 STMicroelectronics – All rights reserved